Lateral viscosity in GOSI9p8 eORCA1

Adam Blaker

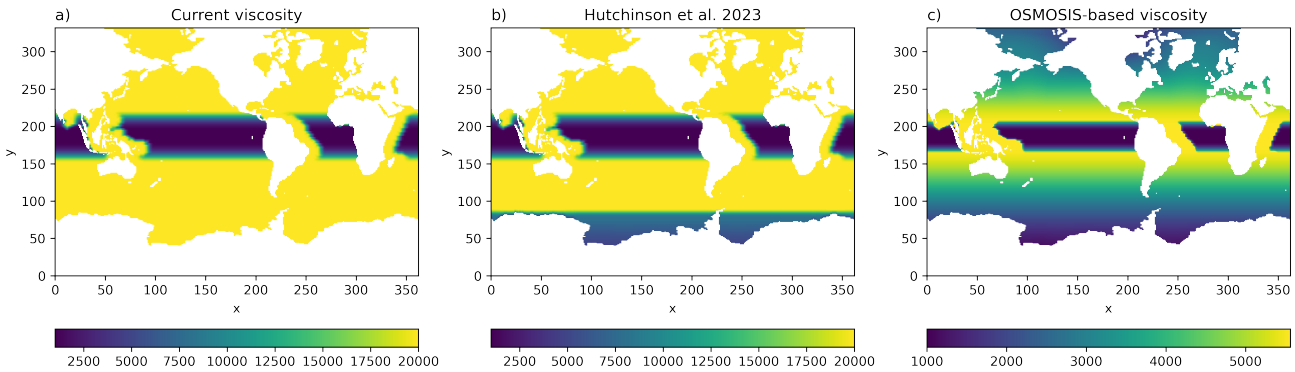

Figure 1: Figure showing the spatial variation of lateral eddy viscosity: a) the current implementation; b) a variant used by Hutchinson et al. (2023) with refinement south of 65°S; c) the OSMOSIS-based implementation with grid-scale dependence

0.1 Background

Although intended to have grid-scale dependent viscosity values consistent with those applied at eORCA025 and eORCA12, a 'feature' of the ldfdyn code resulted in the grid-scale dependent values being overwritten with the reference value 'ahm0' when the equatorial zoom was applied. Early in the GO8 development cycle this lack of grid-scale dependence in both GO6 and GO8 was identified (see here).

Since GO5 (and possibly before?), the eORCA1 configuration has used the reference value of 20,000 m^2/s everywhere except for an equatorial zoom which reduces the values to 1000 m^2/s close to the equator and above 2000 m depth, except along the western boundaries. These values were used in e.g. the CORE-2 intercomparison papers; see Appendix 18 of Danabasoglu et al., (2014).

Development of OSMOSIS began outside of GOX, and instead used the option within NEMO of nn_ahm_ijk_t=20, which sets viscosity dependent on the grid-scale. The OSMOSIS choice of nn_ahm_ijk_t=20, $U_v = 0.084$ gives values for the horizontal viscosity (in m^2/s) of $A_m \sim 4000.\Delta_x/\Delta_0$ where Δ_x is the grid size and Δ_0 is the equatorial grid spacing for the NEMO grid, which seems reasonable assuming one point is sufficient to resolve the Munk boundary layer at the equator (which may or may not be the case).

A 3D eddy viscosity file was created, which combines the values in use by the OSMOSIS configuration and the reduction in viscosity close to the equator and away from the western boundaries. Unfortunately this file did not feed into the future releases of GO8pX. This was realised when recent attempts to open the ice shelf cavities for UKESM2.0 resulted in violations of the viscosity stability criterion

$$A_m < \frac{\Delta_x^2}{2(2\Delta_t)}, \tag{1}$$

where $2\Delta_t$ is the leapfrog time step (Griffies, 2004, eq. 18.18). The default time step for GO8 eORCA1 is 1 hour, so $\Delta_t = 3600s$.

Previous work in 2019 by Pierre Mathiot to open the ice shelf cavities had also revealed the lack of grid-scale dependence when simulations started to violate the viscosity stability criterion. To resolve it Pierre tapered the viscosity at high southern latitudes, starting from 65°S. Hutchinson et al. (2023) use this solution for their study. Mathiot et al. (2017) opened the ice shelf cavities in a GO5-based configuration, but chose a regional 1/4° resolution which uses the grid-scale dependent lateral viscosity.

0.2 Theory

Lateral viscosity must be set high enough constrain the grid Reynolds number (too high and velocity advection dominates accelerations)

$$R = U\Delta_x/A_m < 2, \quad \Rightarrow \quad A_m > \frac{U\Delta_x}{2} \tag{2}$$

and to resolve the frictional boundary layer whose width is given by Munk (1950):

$$L_m = \frac{\pi}{\sqrt{3}}(A_m/\beta)^{1/3}, \tag{3}$$

where β is the planetary vorticity gradient. At coarse resolutions it is the Munk boundary layer resolution that dominates the minimum viscosity constraint (Griffies and Adcroft 2008). The eORCA1 resolution, with its equatorial refinement and quasi-isotropic Mercator projection elsewhere, is (perhaps?) subject to both constraints. Griffies' 2004 book suggests that (p413 eq. 18.28)

$$A_m > \beta(N\Delta_x\sqrt{3}/\pi)^3, \tag{4}$$

where N is the number of gridpoints in the Munk layer, Δ_x is the grid spacing in m, assumed isotropic. Note the π^{-3} factor is substantial. Choosing plausible values for β and f and their variation with latitude gives his Eq. 18.29:

$$A_m > 3.82 \times 10^{-12}(N\Delta_x)^3 cos(\phi), \tag{5}$$

where ϕ is latitude. This gives A_m must be $> 3800m^2/s$ for one grid point at the equator with $\Delta = 100km$, and $A_m > 3800m^2/s.cos(\phi)$ will ensure two grid points in the Munk boundary layer at 60°N. Cherniawsky and Mysak (1989) choose $A_m = 6000m^2/s$ for a 1° x 1.25° "box-ocean" model, on the basis that this gives approximately 2 grid cells within the Munk boundary layer at 30°N.

Setting viscosity too low may not lead to immediate model crashes. It is possible that it will run stably, albeit with large grid-scale noise (checkerboarding), which in turn will lead to an increase in spurious numerical mixing (Griffies and Adcroft 2008). Megann and Storkey (2021) evaluated viscosity in GO6 eORCA025. They found evidence of grid-scale noise with the default viscosity values, and increasing the viscosity led to a reduction in the amount of numerical mixing.

Setting viscosity too high results in poor representation of narrow boundary currents and excessive damping of planetary waves. Both of these issues will lead to slower adjustment of the model towards a steady state (see e.g. Danek et al. 2019). Cherniawsky and Mysak (1989) comment that "If planetary waves are deemed important for model performance, then there does not seem to be any alternative but to lower the eddy viscosity.". Some authors (e.g. Marshall and Johnson 2013 and references therein) argue that boundary wave processes are fundamental process by which the ocean adjusts. Ultimately a viscosity that is too high will violate the stability criterion discussed earlier.

An ideal target would be to set viscosity high enough to limit the level of grid-scale noise, but low enough to enable realistic boundary currents.

Griffies et al. (2000) suggest a sequence of experiments keeping the same grid resolution but increasing the viscosity to ensure that spurious advective mixing is small. They found that two grid points in the Munk boundary layer is sufficient to reduce spurious mixing to a negligible level, though noting that this result may be dependent on MOM's Arakawa 'B' grid implementation.

The reduction of viscosity at the equator as presented in figure 3 appears to violate both the Munk layer and grid Reynolds number constraints. However, note that this is not the case for the Munk layer since the maximum viscosity values are retained within a few degrees of the western boundaries within the domain (see figure 1). For the grid Reynolds number it is less clear. There is significant latitudinal grid refinement between 20°S - 20°N (see figure 2), such that meridional resolution is approximately 1/3°. Mean flow in the equatorial region is extremely anisotropic. The basis for the reduction in viscosity at the equator is Large et al. (2001), who showed much more realistic representation of the equatorial currents in a low viscosity regime.

The viscosity stability criterion that is shaded in figure 3 (upper left) is

$$A_m = 0.3\frac{\Delta_x^2}{4(2\Delta_t)}, \tag{6}$$

which come from rearranging the equation 4.37 in the MITgcm documentation. I'm not sure how the 0.3 which sets the upper limit for stability is determined, though it may be in Adcroft (1995), and the 4 may be specific to the Adams-Bashforth time stepping used in MITgcm.

0.3 Viscosity in NEMO and climate models

A range of options for setting lateral viscosity are available in NEMO, controlled through the parameter nn_ahm_ijk_t. Through this parameter one can specify a spatially constant value, or a range of grid (2D) or grid and depth (3D)

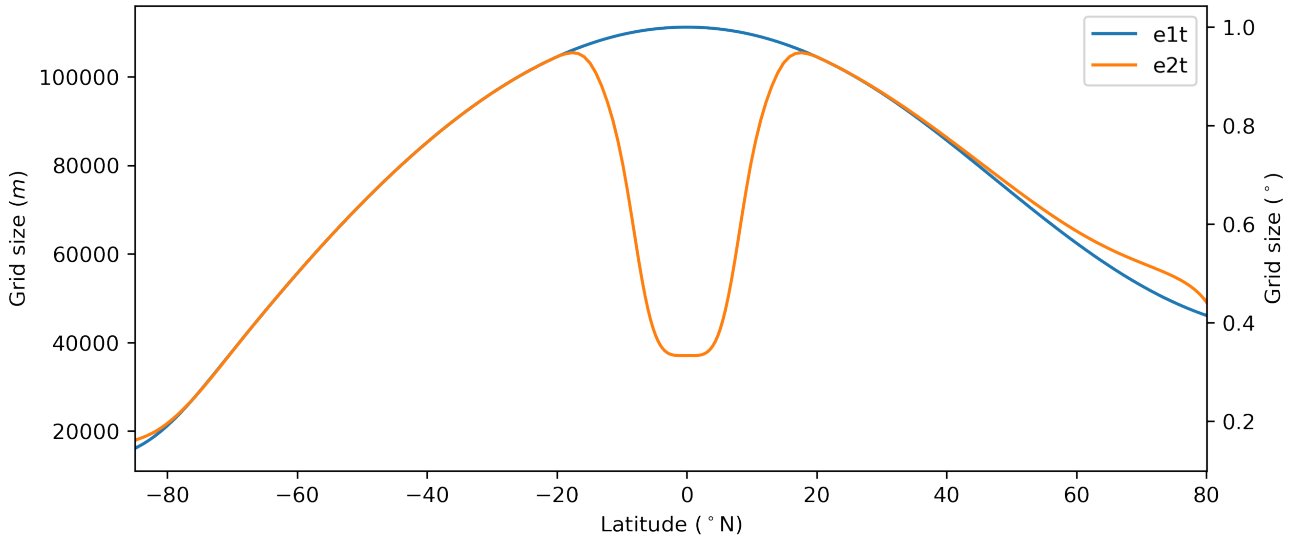

Figure 2: Figure showing the latitudinal variation of the grid size. The cells are quasi-isotropic Mercator, except for the meridional grid refinement at the equator. Note the asymmetry between N and S hemispheres. Grid cells at 80°S are around half the size of grid cells at 80°N, due to the tripolar mesh.

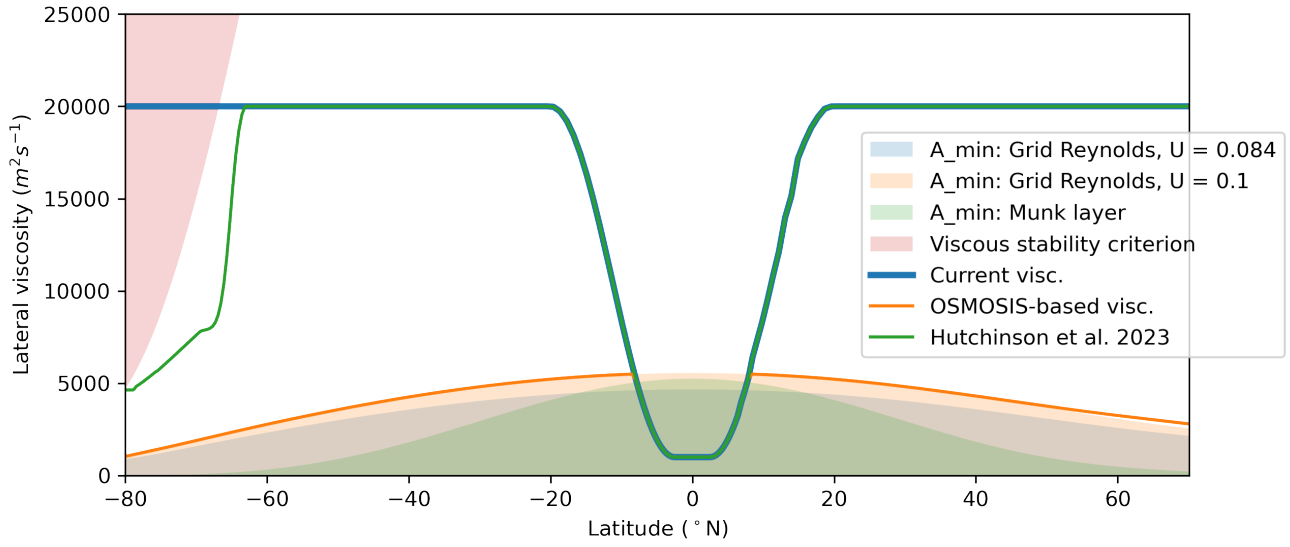

Figure 3: Figure showing the latitudinal variation of lateral eddy viscosity. Lines show the three variations presented in 1. The shaded regions provide: an indication of lower bound required to resolve the Munk layer with one grid cell, and to constrain the grid Reynolds number below 2 given a reference velocity 'U'; and an indication of the upper bound set by the viscosity stability criterion.

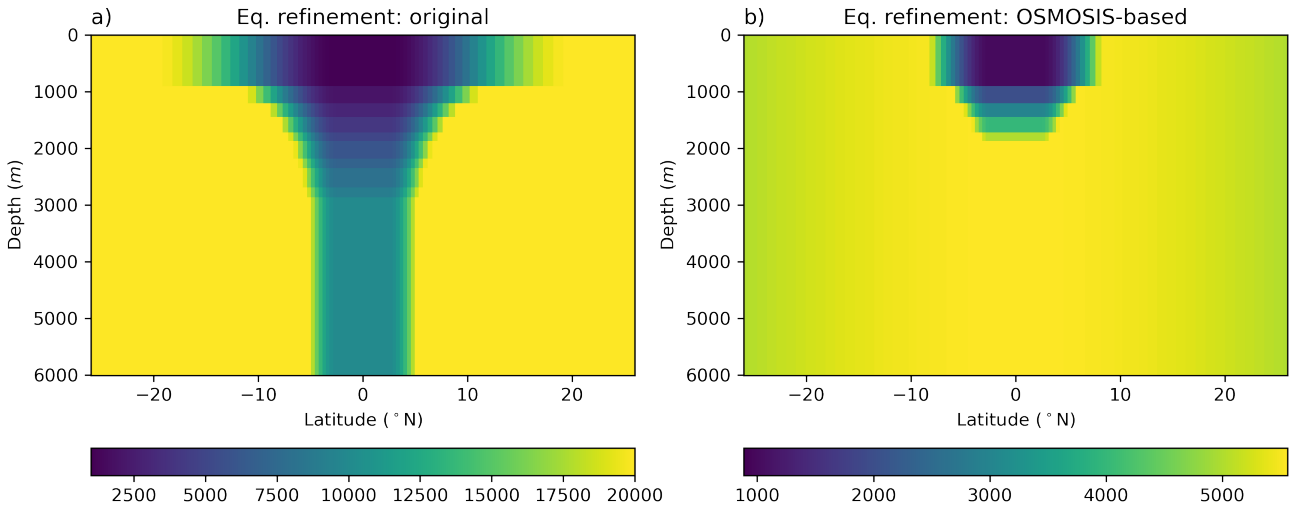

Figure 4: Figure showing the equatorial refinement of lateral eddy viscosity: a) the current implementation and Hutchinson et al. (2023); c) the OSMOSIS-based implementation

dependent values proportional to a reference velocity and length scale. Until NEMO v3.6 there was a hard-coded option to apply a reduction in viscosity close to the equator that is proportional to the meriodional refinement of the grid. From NEMO v4.0 onwards this hard-coded option is removed, and the refinement is applied by supplying a 2D or 3D file that contains the viscosity and diffusivity parameters.

Jochum et al., (2008) compare 3 choices of lateral viscosity and broadly conclude that lower viscosity achieves better representation of many features of the ocean.

A closer relative of GC5, CNRM-CM5.1 (NEMO eORCA1 ocean), uses a uniform value of $1 \times 10^4 m^2/s$ except for a reduction to $1 \times 10^3 m^2/s$ near the equator and away from western boundaries. This is half the value currently set in GO8, with the same equatorial refinement.

0.4 Possible solutions

For GO8, there is a strong desire to apply a latitude dependent viscosity so that consistency across the hierarchy of resolutions is restored. Forced ocean simulations using 3D viscosity file with the OSMOSIS values and the equatorial zoom show a general improvement to most quantities evaluated by marine_assess.

For GC5 and UKESM2.0 there is concern that changing the viscosity at this stage will require the coupled model to be retuned. This will not be possible due to time constraints. Tapering the viscosity at high latitudes in the same/similar way to Pierre Mathiot and Katherine Hutchinson would be a minimally invasive way to enable the opening of ice shelf cavities in UKESM2.0. A similar tapering method was used in Gent et al., 1998 to ensure stability of the NCAR climate model at high latitudes.

We could try higher grid-scale dependent viscosity fields. These would satisfy the desire to maintain consistency with the GO8 hierarchy and, possibly, to negate the need to re-tune the coupled model.

0.5 References

J.Y. Cherniawsky & L.A. Mysak (1989) Baroclinic adjustment in coarse-resolution numerical ocean models, Atmosphere-Ocean, 27:2, 306-326, https://doi.org/10.1080/07055900.1989.9649338

G. Danabasoglu, et al., North Atlantic simulations in Coordinated Ocean-ice Reference Experiments phase II (CORE-II). Part I: Mean states. Ocean Modell., 73(0):76–107, 2014. https://doi.org/10.1016/j.ocemod.2013.10.005

Danek, C., P. Scholz, and G. Lohmann, 2019: Effects of High Resolution and Spinup Time on Modeled North Atlantic Circulation. J. Phys. Oceanogr., 49, 1159–1181, https://doi.org/10.1175/JPO-D-18-0141.1

Gent, P.R., Bryan, F.O., Danabasoglu, G., Doney, S.C., Holland, W.R., Large, W.G., McWilliams, J.C., 1998. The NCAR Climate System Model Global Ocean Component. Journal of Climate 11, 1287-1306.

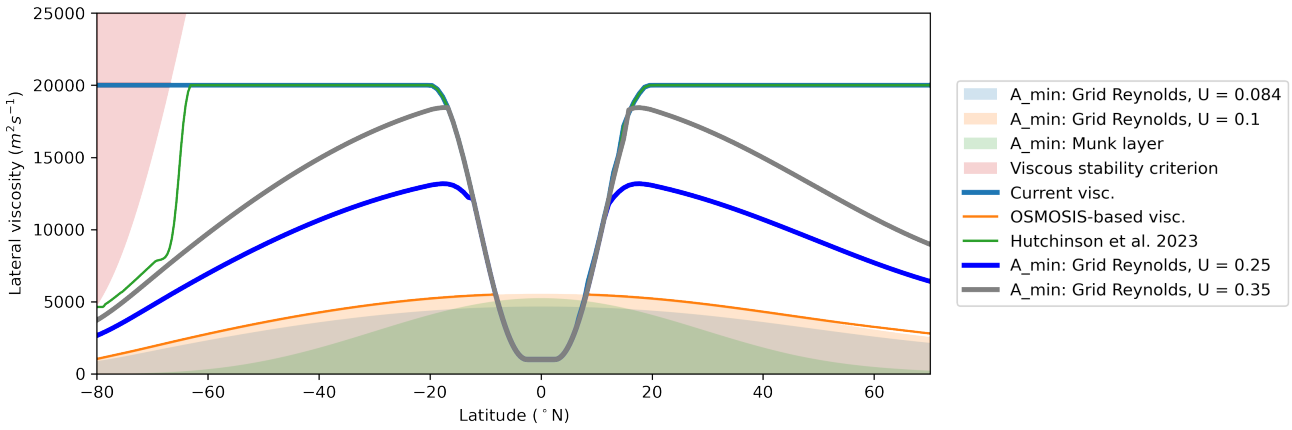

Figure 5: As figure 3 but with two suggestions for higher grid-scale dependent viscosity that use reference velocities 'U' of 0.25 (blue) and 0.35 (grey)

Griffies, S. M., R. C. Pacanowski, and R. W. Hallberg, 2000: Spurious Diapycnal Mixing Associated with Advection in a z-Coordinate Ocean Model. Mon. Wea. Rev., 128, 538–564, https://doi.org/10.1175/1520-0493(2000)128<0538:SDMAWA>2.0.CO;2.

Griffies, Stephen M. Fundamentals of Ocean Climate Models. Princeton University Press, 2004. https://doi.org/10.2307/j.ctv301gzg.

Griffies, S.M. and Adcroft, A.J. (2008). Formulating the Equations of Ocean Models. In Ocean Modeling in an Eddying Regime (eds M.W. Hecht and H. Hasumi). https://doi.org/10.1029/177GM18

Hutchinson, K., Deshayes, J., Éthé, C., Rousset, C., de Lavergne, C., Vancoppenolle, M., Jourdain, N. C., and Mathiot, P.: Improving Antarctic Bottom Water precursors in NEMO for climate applications, EGUsphere [preprint], https://doi.org/10.5194/egusphere-2023-99, 2023.

Jochum, M., Danabasoglu, G., Holland, M., Kwon, Y.-O., and Large, W. G. (2008), Ocean viscosity and climate, J. Geophys. Res., 113, C06017, https://doi.org/10.1029/2007JC004515.

Large, W. G., Danabasoglu, G., McWilliams, J. C., Gent, P. R., & Bryan, F. O. (2001). Equatorial circulation of a global ocean climate model with anisotropic horizontal viscosity. Journal Of Physical Oceanography, 31, 518-536.

Mathiot, P., Jenkins, A., Harris, C., and Madec, G.: Explicit representation and parametrised impacts of under ice shelf seas in the $z*$ coordinate ocean model NEMO 3.6, Geosci. Model Dev., 10, 2849–2874, https://doi.org/10.5194/gmd-10-2849-2017, 2017.

D. P. Marshall and H. L. Johnson. Propagation of meridional circulation anomalies along western and eastern boundaries. J. Phys. Oceanogr., 43(12):2699–2717, 2013. https://doi.org/10.1175/JPO-D-13-0134.1

Megann, A., & Storkey, D. (2021). Exploring viscosity space in an eddy-permitting global ocean model: Is viscosity a useful control for numerical mixing? Journal of Advances in Modeling Earth Systems, 13, e2020MS002263. https://doi.org/10.1029/2020MS002263

MITgcm documentation on numerical stability criteria

Voldoire, A., Sanchez-Gomez, E., Salas y Mélia, D. et al. The CNRM-CM5.1 global climate model: description and basic evaluation. Clim Dyn 40, 2091–2121 (2013). https://doi.org/10.1007/s00382-011-1259-y

Wajsowicz, R. C., 1993: A consistent formulation of the anisotropic stress tensor for use in models of the large scale ocean circulation. J. Comput. Phys.,105, 333–338.